2023 45th Annual International Conference of the IEEE Engineering in Medicine & Biology Society (EMBC) | 979-8-3503-2447-1/23/$31.00 ©2023 IEEE | DOI: 10.1109/EMBC40787.2023.10341187

A custom MR-compatible dataglove for fMRI of the human motor cortex at 7T

Shota Hodono, Jin Jin, Jan Zimmermann, Donald Maillet, David Reutens, and Martijn A. Cloos

Abstract— **We present a custom-built MR-compatible data glove to capture hand motion during concurrent fMRI experiments at 7 Tesla. Thermal and phantom tests showed our data glove can be used safely and without degradation of image quality. Subject-specific Blood Oxygen Level Dependent (BOLD) signal models, for use in fMRI analysis, were constructed based on recorded kinematic measurements. Experiments revealed the relative fMRI BOLD signal contribution of flexing, extending, and sustained isotonic extension. The ability to evaluate subject performance in real-time and create subject-specific BOLD signal models enables a wide range of experimental paradigms with improved data quality.**

Clinical Relevance— **Using an MR compatible dataglove, subject specific Blood Oxygen Signal Level Dependent (BOLD) signal models can be constructed to study how the brain implements fine motor control.**

I. Introduction

Functional MRI (fMRI) at ultra-high field (UHF) provides an elegant framework to study fine motor control. It has contributed to understanding how the human brain processes motor input and output [1]–[3].

Studies investigating motor control require carefully designed paradigms that could benefit from specialized equipment. While sensory cortices are activated by external stimuli, which are often under the direct control of the experimenter; whereas activation in the motor cortex, especially in the primary motor cortex, originates from within the brain itself [4]–[7]. Usually, the fMRI data is analyzed assuming the subjects performed their task perfectly. However, the subject's ability to closely follow the instructions varies with attention and dexterity, introducing deviations from the intended task. In the best case, these will be manifested as small variations in timing. Such experimental flaws can be statistically smoothed out by performing multiple runs of the experiment across multiple subjects. But, in the worst case, subjects may miss (or misunderstand) cues and fail to perform parts of the task. When such problems go unnoticed spurious results may emerge. Implementing dedicated motion tracking devices can help mitigate such experimental confounds.

To monitor subject's task performance, most commonly, cameras are used [8]. However, a large system with multiple cameras is needed to observe the hand from different angles. Such a system views the hand motion from outside the MRI bore. Therefore, the longer the bore of MRI system the narrower viewing angles of the cameras become, which makes motion tracking less accurate. At UHF MRI, the bore is so long and narrow that the hand is generally completely blocked from view. Hence, a wearable motion tracking device is preferred at UHF. A 5DT data glove ultra (Fifth Dimension Technologies) is a commercially available hand tracking device has been used in MRI, and it has helped fMRI researchers to study the human brain motor functions with varieties of experimental designs [6]. However, this device was not specially designed for use in MRI, and its impact on safety and image quality were not evaluated. In addition, the costs of no less than $5,000 and the inability to be synchronized the recorded data with the MR sequence prevent adaptation of this technology by the wider community.

In this paper, we share the design and validation of our custom MR compatible dataglove with ability to synchronize the recoded hand motion with the MR sequence. To exemplify its use, hand motion data collected during concurrent fMRI experiments was used to retrospectively construct signal models for General Linear Model (GLM) analysis, revealing the relative contributions of flexing, extending, and sustained isotonic extension to the fMRI BOLD signal.

II. METHODS

A. MR compatible Dataglove

The dataglove is designed to measure the joint angle of four fingers (not the thumb) using piezo-resistive flex sensors. The resistance of these sensors depends on their bending angle. When mounted on a glove, these sensors encode the joint angle in terms of a change in resistance. The whole dataglove setup is seen in Figure 1.

We built our dataglove around a fire-retardant glove (OMP, Ronco Scrivia, Italy). Cotton pockets were stitched across the proximal interphalangeal (PIP) joints, each holding a piezoresistive flex-sensor (SKU: SEN-1026). The sensors connect to a custom interface-board, holding fuses (TR5 372, 100 mA) and a non-magnetic RJ45 socket. The interface-board was mounted in a 3D-printed housing mounted on the back of the glove using Velcro. A Cat5/6 ethernet cable was used to carry the signals out of the magnet room through a custom-

This works is supported by ARC Future fellowship grant FT200100329. J.Z. is supported by NIH R01EB031765, R56EB031765, P30DA048742, P41EB027061.

S. H., D. M., D.R. and M.A.C. are with Centre for Advanced Imaging, the University of Queensland, St. Lucia, QLD 4072 Australia (s.hodono@uq.edu.au, don.maillet@cai.uq.edu.au, d.reutens@uq.edu.au, m.cloos@uq.edu.au).

J.J. is with Siemens Healthcare Pty Ltd, Brisbane, Australia (jin.jin@siemens-healthineers.com).

J.Z. is with Center for Magnetic Resonance Research, University of Minnesota, Minneapolis, MN 55455, United States (janz@umn.edu).

S.H. is corresponding author (phone: +61-431-828-8887).

built filter panel. The other side of the filter was connected to an Arduino ZERO equipped with a custom interface shield. Each pair of twisted wires connects a single sensor to an ADC which quantifies the joint angle in terms of change in resistance in the sensor. The same interface also recorded the MR trigger signal for synchronization with the MR system. Between the dataglove and the interface box, a filter (LC circuit for each wire) is inserted to prevent RF leaking into the scanner room. The filter was placed in the waveguide tube between MR console room and MR scanner room. All the data are sent to a computer through a serial connection for real-time monitoring and storage.

At the start of each experiment, the dataglove was calibrated for each subject individually. While in the magnet, we asked each subject to stretch their fingers and then make a fist, to identify the sensor values that correspond to angles of 0˚ and 90˚, respectively. The joint angles are then computed assuming a linearly relationship between sensor resistance and joint angle. This assumption and the measurement accuracy was evaluated on bench by comparing actual joint angles and recorded angles.

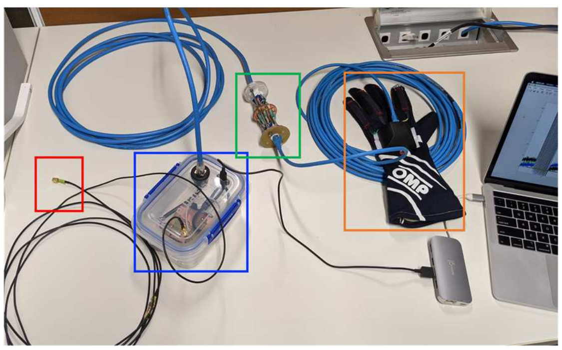

Figure 1: Our custom data glove setup. A SMA connector highlighted by a red box receives trigger signal sent from a trigger splitter. Blue, green and orange boxes show a container holding the interface assembly, the custom-built filter, and MR compatible dataglove respectively. These components were connected through Cat5/6 cables. Flex sensors are inserted into the pockets on the glove (orange box).

B. *Safety assessment*

All components inside the magnet room were first screened for magnetic compatibility, and the complete assembly was checked for RF resonances around the 7 Tesla proton frequency (297Mhz). A range of phantom measurements was performed to ensure safety. Most notably, thermal imaging was used to confirm that neither RF absorption nor fast-switching sequences led to heating (15 min of diffusion-weighted Spin Echo-Echo Planer Imaging (SE-EPI) at >95% SAR reported on console. In the phantom scan, three different configurations were compared; (i) no dataglove, (ii) dataglove with stretched fingers, (iii) dataglove with bend fingers. While scanning, ADC data from the flex sensors were recorded to evaluate interference of the magnetic field gradients to the ADC recording.

C. *Application in functional MRI*

Two healthy volunteers were scanned (38 & 29 yo male). The study was approved by the local human research ethics committee in accordance with national guidelines, and written informed consent was obtained before the scan. All MR experiments were performed at MAGNETOM 7T Pulse system (Siemens Healthcare, Erlangen, Germany) using a 32-channel head coil (Nova Medical, Wilmington, MA, USA).

A SNR map and coil correlation matrix were assessed using the Kellmann method [9] with and without the dataglove. In addition, functional experiments were conducted. Subject 1 was asked to perform periodic flexing fingers motion (left hand only), subject 2 was asked to maintain isotonic extension for ~5 sec before returning back to a comfortable rest position (left hand only). No visual cues were used to guide the timing of subjects' hand movements, and appropriate fMRI signal models were directly derived from the motion measurements by thresholding the first order derivatives (Savitzky-Golay filter) of the joint angle with respect to time. Slice timing and motion correction were performed using SPM12 (Functional Imaging Laboratory, University College London, UK), and the GLM analysis [10] was performed using FSL (https://fsl.fmrib.ox.ac.uk/fsl/) without spatial smoothing or clustering.

A 2D GRE-EPI sequence [11] was used for functional imaging with following parameters; TR = 0.5sec, TE = 24.6ms, flip-angle = 40, 1.1mm isotropic resolution, 18 slices, 143mm x 143mm FOV, GRAPPA = 3 [12], MB = 2, 490 volumes.

III. Results and Discussion

Bench measurements revealed that the angle measurement accuracy was about ± 5˚, when using a sampling rate of ~15Hz per finger. Although a higher accuracy may desirable when studying complex fine motor control tasks, the current angle specificity and temporal resolution are more than adequate to differentiate basic motions commonly used in fMRI studies of motor control, such as finger flexion.

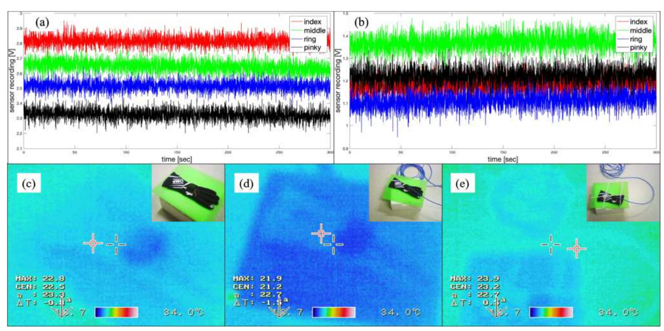

Figure 2: All safety tests were performed with two different positions. Once with the sensors on the dataglove straight and once with the sensors in a bend condition. Panels (a) and (b) show sensor measurements during a 100% SAR diffusion EPI sequence in the straight and bend position, respectively. Panels (c), (d), and (e) show thermal images, before scan, after the scan with straight sensors, and after the scan with bend sensors, respectively.

In vitro B1 mapping and SNR measurements with and without the dataglove showed less than 5% difference. Recoding of the sensors on the glove showed no sign of artifacts from the fast-switching gradients or RF pulses (Fig. 2 a, b). Note that dataglove was placed ~1m away from the head coil. Therefore, it is expected that interaction between the Cat 5/6 cable and transmit B1 fields is minimum. In addition, a twisted pair of wires are used in the Cat 5/6 cable so that each pair of cables has minimal surface with which the magnetic flux of the transmit and gradient fields can couple. Figure 2c-e shows the thermal images obtained pre- and post- high power fast switching sequences. No significant temperature changes were observed (less than 1-degree Celsius change). Thus, the safety tests confirmed that the dataglove can be safely used at 7T MRI without impeding data quality.

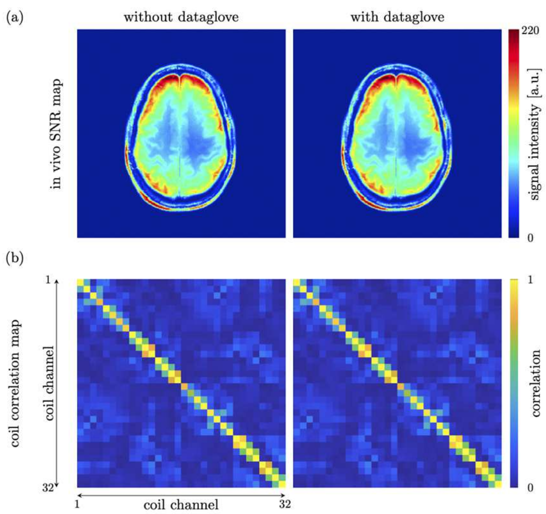

Figure 3: SNR maps (a) and noise correlation matrixes (b) with and without data glove.

In in vivo imaging, no degradation in SNR was observed in the MR images (Fig. 3a). Moreover, the standard deviation of the noise and noise covariance matrix remains nearly identical between scans (Fig. 3b).

Clean kinematic recordings were obtained during fMRI experiments (Fig. 4, 5e). Based on the recorded motion, five different motion states could be identified; (i) flexing, (ii) extending joints, (iii) sustained isotonic extension, (iv) sustained isotonic flexion, and (v) rest (Fig. 4, 5e).

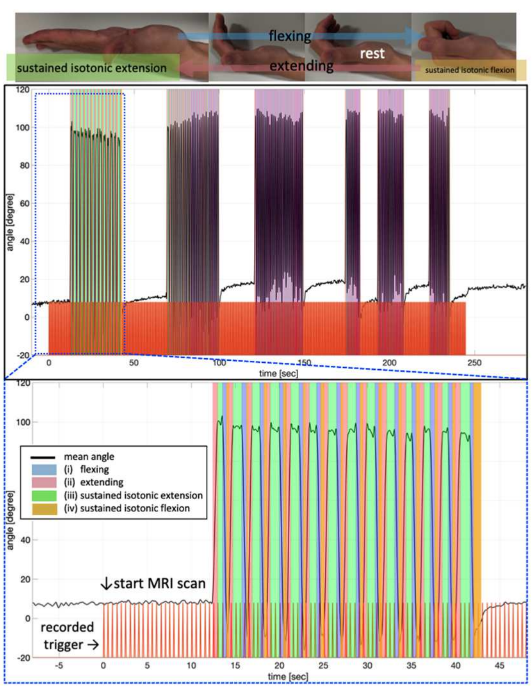

Figure 4. Recorded hand motion during an fMRI scan. The bottom figure shows a zoomed view of the first section. Different motion states are highlighted in the figures. The trigger signal from the MR system is also shown in the figure (orange line).

Figure 5a shows the activation maps from subject 1, generated using our subject-specific signal models. All of the signal models clearly localize the left-hand area on motor cortex (Fig. 5a-c). Looking at the signal dynamics in these voxels, the signal model derived from flexing and extending motions only, showed a reduced amplitude during the first segment in which the fingers maintained isotonic extension for ~2s before flexing (Fig. 5d red). This suggests that holding the maintained isotonic extension significantly contributes to the observed BOLD signal. Figure 5e shows recorded hand motion, the signal models, and the mean signal time series calculated within motor cortex with Z>5, from subject 2 performing a prolonged sustained isotonic flexion (~5sec). The measured BOLD response indeed correlates best with a model that treats the sustained isotonic extension motion states as an active state (Fig. 5e green). In general, specific motor tasks and their associated rate of neuronal activation can have a non-trivial relation which can be further obscured by the hemodynamic response [13]. Iterative modeling of the signal based on precise motion measurement could provide a path forward to study these dynamics in more detail.

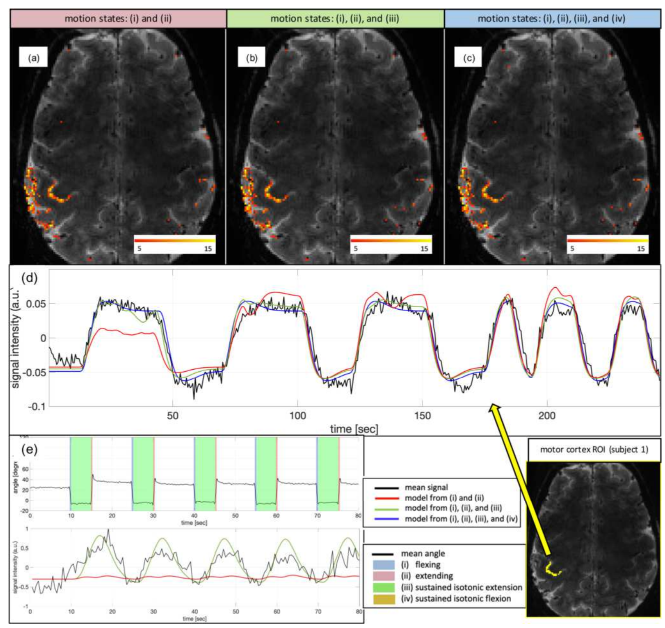

Figure 5. Activation map of subject 1 obtained by GLM using motion states (a) (i) and (ii), (b) (i), (ii) and (iii), (c) (i), (ii), (iii) and (iv). (d) Signal time series and model predictions of subject 1. (e) Recorded hand motion, signal timeseries and model predictions of subject 2. The mean signal time series calculated within motor cortex with Z>5. The figure legend on the bottom right applies for both (d) and (e).

IV. Limitations

Here we used 2.2-inch sensors to measure PIP joints angles. To further improve the angle measurement specificity, shorter sensors can be used to measure distal interphalangeal and metacarpophalangeal joints. Note that we used a CAT 5/6 cable to transfer the analog signal, because the cable contains four twisted pairs of wires which were used to encode analog signals for each finger except thumb. Therefore, if more sensors are added, more cables or other data transfer strategy such as using fiber optics may be required.

If one wants to measure hand kinematics for both hands, extra care must be taken to ensure the subject's safety. Even though there is no direct contact between the subject and electronics, 100mA fuses are used as a fail-safe aimed to avoid potential RF/current burns in the unlikely event of an unforeseen combination of adverse circumstances. However, when two datagloves are used to monitor both right- and left-hand there is a theoretical possibility to create a current loop through the heart, which at select frequencies can be affected by currents as small as 10mA. Therefore, fuses with a lower current rating are advisable in such a setup (~5mA).

V. Conclusion

We presented a custom built MR-compatible dataglove to measure hand motion during concurrent fMRI of the human motor cortex at 7 Tesla without degradation of image quality. The ability to evaluate subject performance in real-time and create subject-specific BOLD signal models enables a wide range of experimental paradigms with improved data quality.

Data sharing

We are happy to share the interface board schematics, Arduino program to operate the dataglove, and the 3D models of the housing mounted on the back of the glove upon request.

Acknowledgment

The authors acknowledge the facilities, and the scientific and technical assistance of the National Imaging Facility at the Centre for Advanced Imaging, University of Queensland.

References

[1] L. Huber et al., "High-Resolution CBV-fMRI Allows Mapping of Laminar Activity and Connectivity of Cortical Input and Output in Human M1," Neuron, vol. 96, no. 6, pp. 1253-1263.e7, 2017, doi: 10.1016/j.neuron.2017.11.005.

[2] L. Huber et al., "Sub-millimeter fMRI reveals multiple topographical digit representations that form action maps in human motor cortex," Neuroimage, vol. 208, p. 116463, 2020, doi: 10.1016/j.neuroimage.2019.116463.

[3] J. C. Siero, N. Petridou, H. Hoogduin, P. R. Luijten, and N. F. Ramsey, "Cortical Depth-Dependent Temporal Dynamics of the BOLD Response in the Human Brain," J Cereb Blood Flow Metabolism, vol. 31, no. 10, pp. 1999–2008, 2011, doi: 10.1038/jcbfm.2011.57.

[4] J. R. Polimeni, B. Fischl, D. N. Greve, and L. L. Wald, "Laminar analysis of 7T BOLD using an imposed spatial activation pattern in human V1," Neuroimage, vol. 52, no. 4, pp. 1334–1346, 2010, doi: 10.1016/j.neuroimage.2010.05.005.

[5] L. D. Lewis, K. Setsompop, B. R. Rosen, and J. R. Polimeni, "Fast fMRI can detect oscillatory neural activity in humans," Proc National Acad Sci, vol. 113, no. 43, pp. E6679–E6685, 2016, doi: 10.1073/pnas.1608117113.

[6] J. C. Siero, D. Hermes, H. Hoogduin, P. R. Luijten, N. Petridou, and N. F. Ramsey, "BOLD Consistently Matches Electrophysiology in Human Sensorimotor Cortex at Increasing Movement Rates: A Combined 7T fMRI and ECoG Study on Neurovascular Coupling," J Cereb Blood Flow Metabolism, vol. 33, no. 9, pp. 1448–1456, 2013, doi: 10.1038/jcbfm.2013.97.

[7] S. Han, S. Eun, H. Cho, K. Uludağ, and S.-G. Kim, "Improvement of sensitivity and specificity for laminar BOLD fMRI with double spin-echo EPI in humans at 7 T," Neuroimage, vol. 241, p. 118435, 2021, doi: 10.1016/j.neuroimage.2021.118435.

[8] J. M. Fernandes, S. Tafula, and J. P. S. Cunha, "Image Analysis and Recognition, 8th International Conference, ICIAR 2011, Burnaby, BC, Canada, June 22-24, 2011. Proceedings, Part II," Lect Notes Comput Sc, pp. 59–67, 2011, doi: 10.1007/978-3-642-21596-4_7.

[9] P. Kellman and E. R. McVeigh, "Image reconstruction in SNR units: A general method for SNR measurement†," Magn. Reson. Med., vol. 54, no. 6, pp. 1439–1447, 2005, doi: 10.1002/mrm.20713.

[10] K. J. Worsley, "Chapter 14, Statistical Analysis of ActivationImages," in Functional Magnetic Resonance Imaging: An Introduction to Methods, 2001. doi: 10.1093/acprof:oso/9780192630711.001.0001.

[11] S. Moeller et al., "Multiband multislice GE-EPI at 7 tesla, with 16-fold acceleration using partial parallel imaging with application to high spatial and temporal whole-brain fMRI," Magnet Reson Med, vol. 63, no. 5, pp. 1144–1153, 2010, doi: 10.1002/mrm.22361.

[12] M. A. Griswold, P. M. Jakob, R. M. Heidemann, M. Nittka, V. Jellus, J. Wang, B. Kiefer, A. Haase, Generalized autocalibrating partially parallel acquisitions (grappa), Magn. Reson. Med., 47 (6), 2002, doi: 10.1002/mrm.10171.

[13] S. Hodono, J. Polimeni, D. Reutens, and M. Cloos, "Tracking rapid stimulus-driven BOLD oscillations in the human primary motor cortex and somatosensory cortex," Proceedings of the Joint Annual Meeting ISMRM-ESMRMB, 2022. 0526.